MACMODS

MacroAlgae Cultivation MODeling System

Macroalgal Growth Model (MAG): Theory

Draft

March 30, 2020

UC Irvine

Kristen Davis (davis@uci.edu)

Christina Frieder (friederc@uci.edu)

UC Irvine

Contents

List of Figures

List of Tables

Introduction

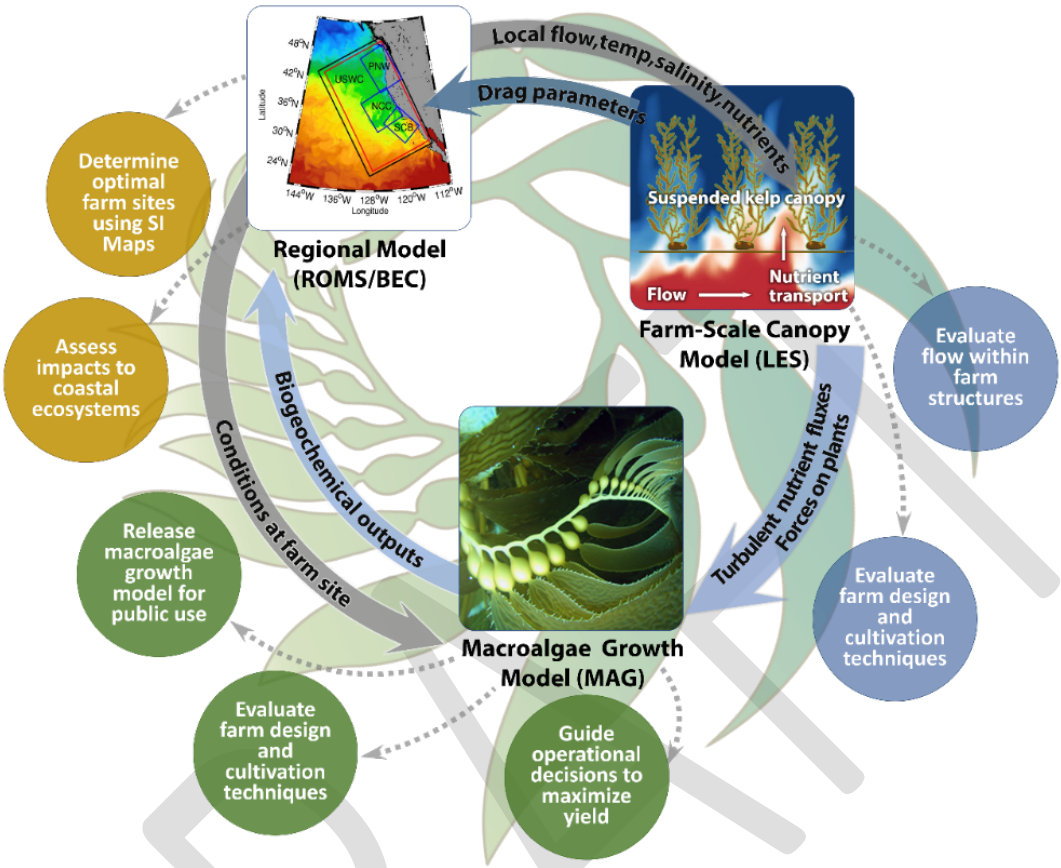

Figure 1. Overview of MACMODS modeling platform.

There are three basic components of the *MACMODS* modelling system: (1) a Regional Ocean Model with biogeochemical fields (ROMS/BEC), (2) a farm-scale hydrodynamic model (large eddy simulation, LES), and (3) a Macroalgal Growth Model (*MAG*).

The purpose of this document is to provide model theory and an in-depth detailing of the MAG model. The model has been initially developed for giant kelp, *Macrocystis pyrifera*, for evaluation of kelp farms off the California coast.

Regional Ocean Conditions

Simulation of offshore macroalgal farms requires knowledge of ocean conditions at the site of interest. This includes standard oceanographic physical, chemical, and biological parameters. Table 1 provides an example list of the environmental conditions required to run MAG and the source of data (modeling and observational) to simulate *M. pyrifera* farms off California.

Table 1. Environmental input parameters for MACMODS (MAG)

Variable	Description	Unit	Source[a]
NO_3	Concentration of nitrate in seawater	µM N	ROMS
NH_4	Concentration of ammonium in seawater	µM N	ROMS
DON	Dissolved organic nitrogen	mM N	ROMS
T	Temperature	Celcius	ROMS
u_x, v_y, w_z	Seawater velocities	m s^{-1}	ROMS
D_z	Vertical diffusivity	m^2 s^{-1}	ROMS, LES
D_h	Horizontal diffusivity	m^2 s^{-1}	ROMS
$def_{u,v}$	Horizontal velocity deficit	nondimensional	LES
T_w	Wave period	s	NDBC
H_S	Significant wave height	m	NDBC
PAR_0	Incoming photosynthetically active radiation	W m^{-2}	ROMS
chl-a	Concentration of chlorophyll-a in seawater	mg Chl-a m^{-3}	ROMS

[a] ROMS = Regional Ocean Model; LES = Large Eddy Simulation; NDBC = National Data Buoy Center

ROMS/BEC

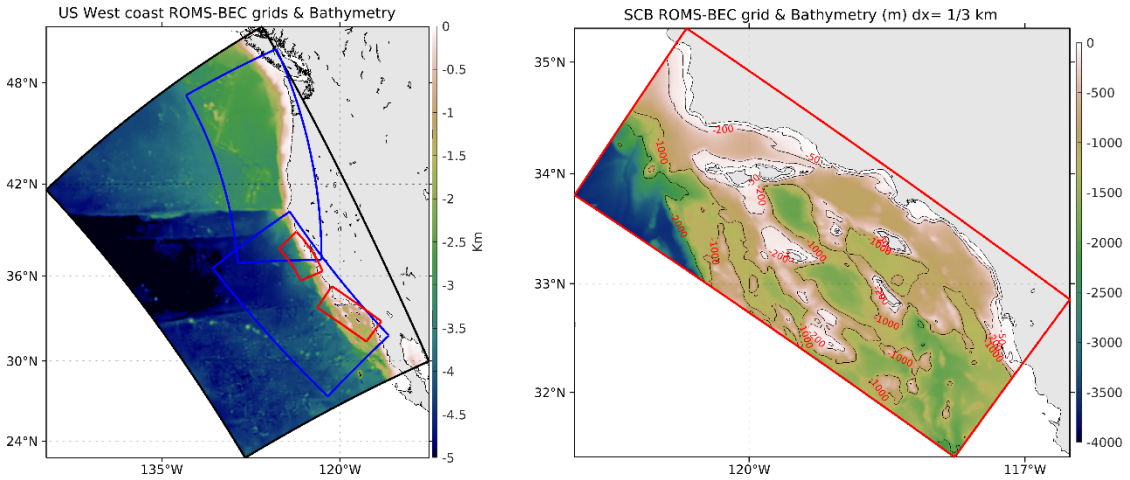

Figure 2. Map of US West Coast ROMS-BEC grid (left) and the ROMS-BEC L2SCB subgrid (right)

The Regional Modeling System (ROMS) is a widely-used, open-sourced code, which has been used for more than a decade in many locations in U.S. coastal waters and elsewhere (www.myroms.org; Shchepetkin and McWilliams 2005). For the U.S. West Coast, the standard model domain spans the entire coast at 4-km resolution, while the large subdomain grids for the southern and northern coastal sectors have 1-km horizontal resolution (Figure 2). The model has a multi-level nesting capability such that the analysis of candidate kelp farms can be done in the region of interest with horizontal resolution of up to 300 m. Ecosystem and biogeochemical dynamics within ROMS are predicted using the ROMS-embedded Biogeochemical Elemental Cycling (BEC) model (Moore et al., 2002; Gruber et al, 2006). BEC includes phytoplankton, zooplankton, dissolved, suspended, and sinking particulates, including four different nutrients (nitrogen, silicic acid, phosphate, and iron). Recent improvements to the ROMS-BEC model of the Southern California Bight (SCB) include the addition of anthropogenic sources of nutrients from wastewater outfalls and riverine sources, which double the estimated amount of available nitrogen in the nearshore of the SCB (Howard et al. 2014). The model includes explicit representations of river sources, sediment chemical fluxes, and particle sinking.

Within-Farm Hydrodynamics (LES)

Offshore cultivation in deeper water requires macroalgae to be grown from suspended structures. This new, emergent-type canopy has potential to generate new flow features that have yet to be computationally or observationally explored. For example, increased currents are likely to occur between the suspended canopy and the ocean floor, increasing bottom stress and creating the possibility of development of shear layer eddies below the canopy (Plew 2011). If shear layer eddies develop, they could increase drag forces acting on the plants and farm structure. They are also likely to increase the mixing of nutrient-rich water into the canopy region. We implement a fine-scale turbulence model to assess how flow attributes, hydrodynamics forces, and nutrient availability respond to different farm designs and cultivation techniques.

LES parameterization and output

LES utilizes leaf area index (LAI; $m^2\ m^{-3}$) to estimate drag forces by kelp exerted on flow. Values of LAI are depth resolved and derived from the 1-d version of MAG. Given computational limitations, a subset of kelp and boundary condition scenarios have been selected for LES simulation (Table 2). There are two LAI scenarios: “subsurface” and “max canopy.” The “subsurface” is defined as the last day before the kelp reaches the surface (e.g., max amount of subsurface biomass, but biomass in canopy is zero). The “max canopy” is defined as the day there is the maximum amount of biomass in the canopy portion.

LES synthesizes flow fields into time-averaged, spatially varying velocity deficits for each dimension (x, y, and z) as well as a spatially varying vertical diffusivity estimate.

Table 2. LES simulations and parameterization

	ID	CANOPY TYPE	CULTIVATION DEPTH	FARM DESIGN	FLOW*
"BASE CASE"	1a	subsurface	20	Backbone	parallel
	1b	max	20	Backbone	parallel
BLOCK	2a	subsurface	20	Block design	parallel
	2b	max	20	Block design	parallel
CULT. DEPTH	4a	subsurface	10	Backbone	parallel
	4b	max	10	Backbone	parallel
PLANT DENSITY	5a	subsurface	20	Backbone/2	parallel
	5b	max	20	Backbone/2	parallel
FLOW	6a	subsurface	20	Backbone	perpendicular
	6b	max	20	Backbone	perpendicular

Macroalgal Growth Model (*MAG*)

State Variables

The Macroalgal Growth Model (*MAG*) tracks nitrogen in six pools: ammonium (NH_4), nitrate (NO_3), dissolved organic nitrogen (DON), particulate organic nitrogen (PON), stored nitrogen in macroalgae (N_s), and fixed nitrogen in macroalgae (N_f; Figure 3). The currency of nitrogen has been selected as this is, most often, the nutrient limiting autotrophic productivity, particularly along the U.S. West Coast (Eppley et al. 1979; including for kelp, Zimmerman and Kremer 1984, 1986).

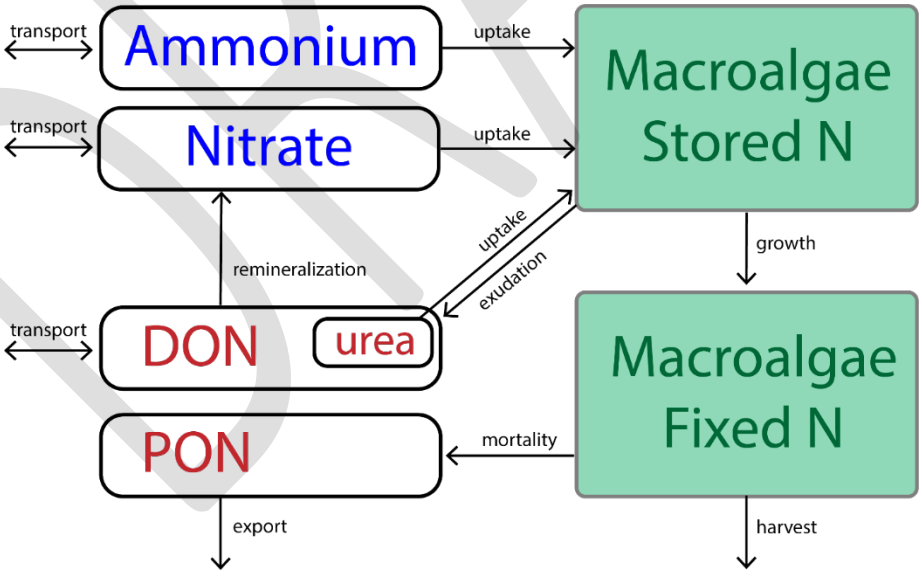

Figure 3. Macroalgal Growth Model

Distinguishing between two pools of internal nitrogen (stored and fixed; N_s and N_f) is based on Droop's cell quota model (Droop 1983) in that growth depends on the internal level of the

limiting nutrient (nitrogen). The nutrient quota, Q, is defined as the relative mass of nitrogen per unit of biomass (Equation 1). There is a minimum amount of relative nitrogen required for life, referred to as "critical tissue N content" or Q_{min} (mg N g-dry^{-1}). Q_{min} is used as a conversion ratio between nitrogen content and biomass (Equation 2).

Equation 1

$$Q = Q_{min}\left(1 + N_s/N_f\right)$$

Equation 2

$$\mathrm{B} = N_f/Q_{min}$$

Macroalgal Forms Simulated by *MAG*

Macroalgae generally refers to macroscopic forms of algae (not true plants) found in brackish and sea water. Macrophytes can vary substantially in their morphology and habitat requirements, and where the organism occurs in the water column impacts *MAG* model formulation. For example, a macroalgal type that grows at a single depth – and is not canopy forming – interacts with the environment in a much different manner than macroalgae that extends vertically through the water column and is canopy forming.

MAG setup has been designed to be flexible and easily adapted to many types and species of macroalgae. Initially we have developed and parameterized *MAG* for giant kelp, *Macrocystis pyrifera*. *M. pyrifera* undergoes alternation of generations. It is the sporophyte stage that is the conspicuous, and foundational, member of kelp forests. The sporophyte anchors itself to substratum via a holdfast and grows via extension of fronds from the holdfast (Figure 4). Growth occurs apically by generating new blades at the tip of the frond. Each blade is attached to the stipe via a gas bladder, making the algae buoyant. Individual fronds grow rapidly – up to 0.5 m d^{-1}, can reach 25+ m in length (Clendenning 1971), and senesce after a few months while whole plants can persist for many years (Rodriguez et al. 2013). New fronds are continually initiated at the holdfast.

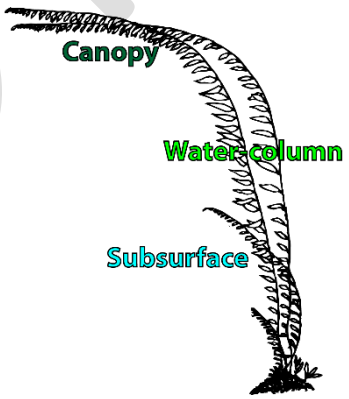

Figure 4. Schematic of M. pyrifera *with subsections labeled.*

For *M. pyrifera*, *MAG* tracks the growth and senescence of individual fronds during the sporophyte stage. Holdfasts are not included in the model, as they contribute little to uptake and growth (Gerard 1982 JEMBE). Sporophylls, or reproductive fronds, are also not included in the model as they extend only a few meters from the bottom and make negligible contribution to growth relative to growing fronds (Arnold and Manley 1985), and thus also contribute little to potential harvestable biomass.

While the model tracks pools of nitrogen between the environment and the macroalgae, the amount of macroalgae can be represented in units other than nitrogen: wet biomass, dry biomass, nitrogen mass, and surface area. Conversion among these units is based on allometric relationships that have been established for *M. pyrifera* (Table 3). These allometric relationships are not uniform across the length of the frond. For example, more biomass is often concentrated near the growing edge of fronds (North 1979), and so allometric relationships are applied based on the portion of the frond (following Rassweiler et al. 2018) (Figure 4). (1) "Subsurface" identifies a frond that has not reached the surface. Fronds that have reached the surface are treated in two sections – (2) the "Water-column" section is the portion of frond that is underwater stretching from the holdfast to the sea surface, and (3) the "Canopy" section is the portion of the frond that floats at the sea surface.

Table 3. Conversion constants used to express amounts of Macrocystis pyrifera

Relationship	Plant section	Units	Conversion	Reference
Dry-to-Wet Weight		g-dry g-wet^{-1}	0.094	Rassweiler et al. 2018
Weight-to-Length	Subsurface	kg-wet m^{-1}	0.117	Rassweiler et al. 2018
	Water-column	kg-wet m^{-1}	0.105	Rassweiler et al. 2018
	Canopy	kg-wet m^{-1}	0.259	Rassweiler et al. 2018
Surface Area-to-Weight	Subsurface	cm^2 g-wet^{-1}	32.2	Haines and Wheeler 1978
	Water-column	cm^2 g-wet^{-1}	10.9	Fram et al. 2008
	Canopy	cm^2 g-wet^{-1}	58.7	Fram et al. 2008
N_f-to-Length ($N_{f\text{-capacity}}$)	Subsurface	mg N m^{-1}	109.98	derived [a]
	Water-column	mg N m^{-1}	98.7	derived [a]
	Canopy	mg N m^{-1}	243.46	derived [a]

[a] N_f-to-length conversion derived from Weight-to-Length relationship.

State Equations for N_s and N_f

Macroalgal growth is modeled as a two-step process. First, nitrogen is taken up from seawater into an internal reserve of stored nitrogen (N_s; mg N m^{-3}). N_s is converted into fixed nitrogen via growth (N_f; mg N m^{-3}), resulting in increased macroalgal biomass (B; g-dry m^{-3}) (Equation 3 & Equation 4).

Equation 3

$$\frac{\partial \mathrm{N_s}}{\partial \mathrm{t}} = \mathrm{U} \times \mathrm{B} - (G + E + M + H) \times \mathrm{N_s}$$

The change in N_s over time is attributable to uptake of nitrogen from seawater (U; mg N g-dry^{-1} d^{-1}), growth (G; d^{-1}), exudation (E; d^{-1}), mortality (M; d^{-1}) and harvesting (H; d^{-1}). N_s is calculated for each depth bin along the length of the frond (e.g., dz = 1 m).

Translocation of N_s

Translocation is a physiological phenomenon by which N_s can be redistributed vertically along the length of the frond. Translocation occurs through a network of sieve tubes that are located at the center of stipes and into blades, and rates of translocation occur on the scale of multiple meters per day (Schmitz and Lobban 1976; Parker 1966). For macroalgae that inhabit large vertical gradients (such as *M. pyrifera*), translocation enables the growing edge of the plant to exploit higher nutrient concentrations near the base of the plant. To account for this process in the model, the change in N_s at a given time step is summed across the entire frond and redistributed based on the vertical distribution of fixed nitrogen. Computationally, this results in a uniform distribution of Q along the length of the frond which corresponds with field observation that nitrogen content of blades along the frond exhibit little variation (Rassweiler et al. 2018).

Equation 4

$$\frac{\partial \mathrm{N_f}}{\partial \mathrm{t}} = \mathrm{G} \times \mathrm{N_s} - (M + H) \times \mathrm{N_f}$$

The change in N_f over time is due to growth (G; d^{-1}), mortality (M; d^{-1}), and harvesting (H; d^{-1}).

Apical growth of N_f

The change in N_f is calculated for each depth bin along the length of the frond (e.g., dz = 1 m), but growth is apical in macroalgae (occurs at tip of extending frond). To account for apical growth, growth and mortality occurs at every depth along the length of the frond, but changes in N_f due to these two processes are redistributed towards the surface. The amount of N_f within any given depth bin is set by a capacity term ($N_{f\text{-capacity}}$; mg N m^{-1} frond). The determination of $N_{f\text{-capacity}}$ is based on allometric relationships between biomass and length (Table 3). There is no limit to the amount of N_f that can accumulate in the canopy portion. Although, growth does cease once the maximum frond height (h_{max}) is reached (see *Growth*).

The subsurface portion of macroalgae grows vertically through the water column (i.e., maintains position in x and y). Once the plant reaches the surface it accumulates at the surface layer as 'canopy.' Biomass in the canopy is redistributed horizontally based on the average length of the canopy portion of the fronds using a uniformly weighted smoothing function. This feature is important for two processes: modification of nutrient fields at the surface of the ocean due to macroalgal uptake and attenuation of light through the water column due to macroalgal shading.

Process Formulas for N_s and N_f

Uptake

The uptake of nitrogen from seawater is derived from multiple nitrogen sources. For *Macrocystis pyrifera*, nitrogen sources have been demonstrated for nitrate, ammonium, and urea (Gerard 1982; Haines and Wheeler 1978; Smith et al. 2018). The total nitrogen uptake rate (mg N g-dry^{-1} d^{-1}) is the sum of the uptake rates of each nitrogen source. A summation, as opposed to preferential or hierarchical uptake, has been empirically demonstrated (i.e., the presence of one nitrogen source doesn't depress the uptake of another nitrogen source; Haines and Wheeler 1978). Nitrogen transport occurs across the membranes of cells predominately at the blade with little to no contribution from the stipe or holdfast (Gerard 1982). Because of this, uptake rates are computed from surface area-specific fluxes for blades only, and this is then converted to mass-specific values.

The maximum uptake rate of a given nutrient, $U_{max,i}$ (µmol N m^{-2} d^{-1}), can be limited by both physical and biological factors. Those that have been studied for *M. pyrifera* include substrate concentration (e.g., Michaelis-Menten kinetics), mass-transfer limitation due to hydrodynamics (e.g., diffusion boundary layers), light, depth, nutritional history, tissue age, and position in tissue. Substrate concentration is the most important parameter influencing uptake rate (*en sensu* Gerard 1982; Michaelis-Menten kinetics). Nutritional history also has a strong influence on uptake rates; macroalgae have significant nitrogen storage capacities that reflect past nutrient supplies that can lead to an uncoupling between seawater nutrient concentration and uptake rate (Droop 1973, 1983; Hurd 2000). In *M. pyrifera*, nitrogen uptake rate decreases in tissue that has been exposed to nitrogen-replete conditions (Kopczak 1994).

There have been conflicting results of the influence of light and depth and so are not included in the model (Gerard 1982; Kopczak 1994). Tissue age and position along the blade have not been observed to influence uptake rates and so are also not included (Gerard 1982).

The final formulation of uptake is both kinetic and mass-transfer limited, as well as dependent on internal nutrient quota and tissue type.

Equation 5

$$\mathrm{U} = \sum_{i=1}^{3} \mathrm{U_{max,i}} \left[\mathrm{f(C_i, |u|, T_w)} \times \mathrm{f(Q)}\right] \times \frac{Area}{DW} \times \frac{Blade}{Frond} \times \frac{2\ sides}{Blade}$$

where, C_i is the concentration of the constituent nutrient in seawater, $|u|$ and T_w are the magnitude velocity and wave period, respectively, and Q is the internal nutrient quota. The limitation of uptake due to kinetic and mass-transfer limitations was adapted from Stevens and Hurd (1997). Essentially, it is a Michaelis-Menten parameterization of uptake that is depressed by slowed flow thickening the diffusive boundary layer. Uptake is then

replenished by wave action that acts by stripping away the diffusive boundary layer. This functional response is expressed as:

Equation 6

$$f(C_i, |u|, T_w) = \frac{C_i}{K_{m,i}\left(\frac{C_i}{K_{m,i}} + \frac{1}{2}\left(\gamma + \sqrt{\gamma^2 + 4\frac{C_i}{K_{m,i}}}\right)\right)}$$, where

Equation 7

$$\gamma = 1 + \frac{V_{max,i}}{\beta K_{m,i}} - \frac{C_i}{K_{m,i}}$$

where, $K_{m,i}$ is the half saturation constant and $V_{max,i}$ is the maximum uptake rate for nutrient *i* (Table 6). These parameters have been estimated for each nutrient from both laboratory and *in situ* time-course experiments (Table 6; see notes regarding estimation of urea uptake parameters). β in the above formulation is the sum of two terms:

Equation 8

$$\beta = \frac{D}{\delta_D} + \frac{4\delta_D}{T_w}\sum_{n=1}^{\infty}\left(\frac{1 - \exp\left(\frac{-Dn^2\pi^2 T_w}{2\delta_D^2}\right)}{n^2\pi^2}\right)$$

The first term represents mass-transfer limitation due to the presence of a diffusion boundary layer, δ_D, and the second term represents the stripping away of the diffusion boundary layer twice each wave period, T_w. D is the molecular diffusion coefficient (D = T * $3.65 \times 10^{-11} + 9.72 \times 10^{-10}$ m^2 s^{-1}; Li and Gregory 1974). The upper limit of summation was optimized to save on computational time yet still attain at least 95% of summation when set to 1000. This value was determined to be 25. The diffusion boundary layer thickness, δ_D, is modeled as an empirical function of the magnitude velocity (m s^{-1}; Stevens and Hurd 1997).

Equation 9

$$\delta_D = 10\frac{\nu}{0.33|u|}$$

The kinematic viscosity, *v*, is 10^{-6} m^2 s^{-1} (REF). The high coefficient of 0.33 has been argued to be required for δ_D to match whole-frond drag estimates at low velocities (Stevens and Hurd 1997).

The limitation of uptake due to internal nutrient reserves is based on the observation that macroalgae have nitrogen storage capacities that reflect past nutrient supplies (Hurd 2000). Such luxury uptake is formulated with the Droop equation (Droop 1974; Solidoro

et al. 1997) in which there is a minimum internal nutrient level (Q_{min}) at which uptake is maximized and a maximum internal nutrient level (Q_{max}) at which uptake ceases:

Equation 10

$$f(Q) = \frac{Q_{max} - Q}{Q_{max} - Q_{min}}$$

Growth

Nitrogen is converted from N_s to N_f through macroalgal growth (G). The maximum growth rate, G_{max} (d^{-1}), is limited by temperature (T), availability of photosynthetically active radiation (E), and internal nutrient reserves (Q). Growth ceases when the maximum attainable frond height, h_{max} (m), is reached.

Equation 11

$$G = G_{max}[f(T) \times f(E) \times f(Q)]$$

Temperature

Macrocystis sporophytes exist across a broad range of temperature, but do not survive well in very cold or very warm waters (Schiel and Foster 2015). In the field, growth rates have been observed to be independent of temperature below 21 °C (Zimmerman and Kremer 1986). The temperature limitation on growth is expressed as a piecewise formulation (see Table 6 for parameter values):

Equation 12

$$f(T) = \begin{cases} (T_{min})^{-1} \times T, & T < T_{min} \\ 1, & T_{min} \leq T < T_{max} \\ (T_{max} - T_{lim})^{-1} \times T + (T_{max}/T_{lim} + 1)^{-1}, & T_{max} \leq T < T_{lim} \\ 0, & T \geq T_{lim} \end{cases}$$

Light

As primary producers, photosynthetically active radiation (PAR) is essential for photosynthesis and thus growth. We have selected a formulation of the effect of PAR (E) on growth rates derived from field-based transplant experiments of juvenile *Macrocystis* that were fit with a von Bertalanffy growth equation (Dean and Jacobsen 1984). After modification of the above experimental data to relative growth rates based on G_{max}, our modified formula is:

Equation 13

$$f(E) = \begin{cases} 0, & PAR < PAR_c \\ 1 - exp[k_{PAR}(PAR - PAR_c)], & PAR \geq PAR_c \end{cases}$$

k_{PAR} is the light-limited growth constant. PAR_c is the value at which growth ceases, known as the light-limited compensating irradiance (W m^{-2}). For PAR < PAR_c, f(E) = 0. Thus, growth is either zero or positive, but never negative as mortality is explicitly modeled in *MAG*.

Nutrient reserves

The growth limitation due to nutrient reserves also takes a Droop formulation in which growth is maximized when the internal nutrient quota reaches Q_{max} and minimized as the internal nutrient quota reaches Q_{min}. It takes the formulation of:

Equation 14

$$f(Q) = \frac{Q - Q_{min}}{Q_{max} - Q_{min}}$$

Exudation

Exudation is the loss of dissolved material to the surrounding environment and is only derived from the stored pools (e.g., N_s). It has been well demonstrated to be an important loss term in macroalgae, including *Macrocystis*. However, it is typically expressed and considered in terms of carbon loss or total organic loss, and not as nitrogen loss. It is unclear what fraction of exudation is nitrogen. In Hadley et al. (2015), N_s is lost to seawater as ammonium via mortality terms and excludes any loss due to exudation. Exudation is included in the Broch and Slagstad (2012) model in the carbon component only; carbon reserves are lost via exudation proportional to the size of the carbon reserves (as an exponential functional response), and there is no loss term for stored nitrogen.

In the present form of our model, N_s is lost to the dissolved organic nitrogen pool via exudation. The exudation rate is based on field observations (Table 6; Rassweiler et al. 2018) and is set to be constant. However, field studies have also found that the release of dissolved organic matter by *Macrocystis* varies as a function of irradiance and tissue type (Reed et al. 2015). Blade loss is 2.5 times the rate of stipe mass, and exudation is greater under high light versus low light conditions. The functional response (not implemented in our model) is: $d_{blade} = 4.90 \times 10^{-4} + 1.66 \times 10^{-5} \times PAR$; $d_{stipe} = 0.39 \times d_{blade}$

Mortality

There are both intrinsic and extrinsic sources of mortality.

a. Intrinsic mortality is represented as age-dependent mortality. Because we are tracking fronds in the model, age-dependent mortality is specific to fronds. While whole plants of *Macrocystis* can live 3-7 years, fronds have a life span on the scale of months (Rodriguez et al. 2013). In the field, there is a distribution of observed frond life spans, but we have selected an upper value (Age_{max} = 150 d; Table 6) since there are other sources of mortality also included in our model that contribute to loss prior to age-dependent senescence.

b. There are both biological and physical contributors to extrinsic mortality. The sources of biomass loss included in *MAG* are wave-induced losses (d_{wave}) and blade-erosional losses (d_{blade}). d_{wave} is wave-dependent loss and is a function of the significant wave height, H_s (m; Table 6). d_{blade} is a loss rate attributable to continual deterioration observed for blades. Therefore, it is only applied to the proportion of frond that is blade (Table 6; note, a fraction of d_{blade} could be considered as intrinsic mortality since blades have a shorter lifespan than fronds; Rassweiler et al. 2018). d_{frond} is the rate of loss following age-based mortality or harvest-based mortality. Mortality is applied to both stored and fixed nitrogen pools. Other sources of mortality not included in the model include, for example, whole-plant mortality, cutting of fronds due to boating activities, and grazing. In an offshore, suspended canopy loss due to grazers is uncertain.

Equation 15

$$M = \begin{cases} d_{wave} + d_{blade} \times \dfrac{Blade}{Frond}, & Age < Age_{max} \\ d_{frond}, & Age \geq Age_{max} \end{cases}$$

Frond Initiation

New fronds are initiated (d^{-1}) as a function of the nitrogen status (Q) of existing fronds given that light at depth is greater than the compensating light irradiance, PAR_c (T. Bell, pers. comm.).

Equation 16

$$S_i = \begin{cases} 0, & PAR_{z=cult.depth} \leq PAR_c \\ 0.0042 \times Q + 0.17, & PAR_{z=cult.depth} > PAR_c \end{cases}$$

Harvest

Harvesting ($H_{t,x,y,z}$; d^{-1}) of *Macrocystis* entails removing the canopy portion of fronds while the holdfast and subsurface fronds stay intact. Portions of the frond that remain post cutting (e.g., subsurface) senesce at a rate of d_{frond}, while fronds that were subsurface and not cut will continue to grow and regenerate a new canopy.

State Equations for External Inorganic Nutrients

Modeling dissolved inorganic nitrogen in both nitrate and ammonium forms allows for the distinction between potentially very different nutrient sources: i.e., nitrate delivery via wind-driven upwelling of nutrients versus ammonium from wastewater treatment effluent or output from finfish aquaculture. In natural macroalgal beds, there is also clear evidence for regenerated nitrogen from benthic macrofauna, macroalgal epibionts, and fish (Hurd et al. 2000; Hepburn and Hurd 2005; Fram et al. 2008; Peters et al. 2019).

Nitrate

Equation 17

$$\frac{\partial \mathrm{NO_3}}{\partial \mathrm{t}} = Diffusion - Advection - U_{NO_3} \times \mathrm{B} + Remin \times [DON]$$

Ammonium

Equation 18

$$\frac{\partial \mathrm{NH_4}}{\partial \mathrm{t}} = Diffusion - Advection - U_{NH_4} \times \mathrm{B}$$

The change in inorganic nitrogen within the farm is due to transport via advection and diffusion and to loss via uptake by macroalgae. See Section – *Transport of Constituent Nutrients*. In the above formulation there is no contribution to ammonium via regenerated nitrogen (e.g., from benthic macrofauna, fish, etc.). This can be incorporated by adding an additional Source term to Equation 18.

State Equations for External Organic Matter

Dissolved Organic Nitrogen

Modeling dissolved organic nitrogen (DON) allows for the evaluation of macroalgal exudate in the environment. Additionally, organic nitrogen also contributes to macroalgal growth (Harrison and Hurd 2001). In macroalgae, urea (a constituent of the DON pool) can be taken up by macroalgae and reduced to ammonium via the enzyme urease. The fraction of dissolved organic nitrogen that is urea is variable in coastal environments, but on average is 20% (Bronk 2002). We use [Urea] = [DON] × 0.2 as an estimation to the concentration of organic nitrogen available for uptake by macroalgae.

Equation 19

$$\frac{\partial DON}{\partial \mathrm{t}} = Diffusion - Advection - U_{DON \times 0.2} \times \mathrm{B} + (E + M) \times N_s - Remin \times [DON]$$

The change in DON within the farm is due to transport via advection and diffusion, macroalgal uptake (sink) macroalage exudation and mortality from the N_s pool (source), and remineralization that converts DON back to nitrate (sink).

Particulate Organic Nitrogen

Particulate organic nitrogen (PON) from macroalgae accumulates via mortality losses.

Equation 20

$$\frac{\partial PON}{\partial \mathrm{t}} = \mathrm{M} \times N_f$$

Transport of Constituent Nutrients

Constituent transport for dissolved or suspended materials is based on the 3-D advection and diffusion equation to which source and sink terms have been added (Equation 21).

Equation 21

$$\frac{\partial C}{\partial t} = -\frac{\partial (uC)}{\partial x} - \frac{\partial (vC)}{\partial y} - \frac{\partial (wC)}{\partial z} + \frac{\partial}{\partial x}\left(D_h \frac{\partial C}{\partial x}\right) + \frac{\partial}{\partial y}\left(D_h \frac{\partial C}{\partial y}\right) + \frac{\partial}{\partial z}\left(D_v \frac{\partial C}{\partial z}\right) \pm S$$

where, C is the concentration of the nutrient being transported; u, v and w the velocities in the x, y, and z direction; D_h and D_v are horizontal and vertical turbulent diffusion coefficients (Table 4); S is the source/sink term specific to each nutrient.

Table 4. Source of advection and diffusion terms used by MAG transport function

Term	Description	ROMS-informed transport	LES-informed transport
u	x-component of advection	$u_{MAG(x,y,z)} = u_{ROMS(z)}$	$u_{MAG(x,y,z)} = \Delta u_{LES(x,y,z)} \times u_{ROMS<z>} + u_{ROMS<z>}$ <z>: vertically averaged
v	y-component of advection	$v_{MAG(x,y,z)} = v_{ROMS(z)}$	$v_{MAG(x,y,z)} = \Delta v_{LES(x,y,z)} \times v_{ROMS<z>} + v_{ROMS<z>}$
w	z-component of advection	$w_{MAG(x,y,z)} = 0$	$w_{MAG(x,y,z)} = \Delta w_{LES(x,y,z)} \times u_{ROMS<z>}$
D_v	vertical diffusivity	$D_{v,MAG(x,y,z)} = D_{v,ROMS<z>}$	$D_{v,MAG(x,y,z)} = D_{v,LES(x,y,z)} \times u^* \times h_c$ u^*: surface friction velocity h_c: canopy height
D_h	horizontal diffusivity	0.02 m^2/s	0.02 m^2/s

In *MAG*, the numerical solution for the three-dimensional transport equation implements the alternating direction implicit (ADI) method. The method is fully implicit for diffusion due to its parabolic nature, and fully explicit for advection due to its hyperbolic nature. The discretization scheme for diffusion is first-order central differencing and for advection is upwind differencing after an evaluation of flow direction. See Appendix for more detail.

Attenuation of Light Due to Macroalgal Shading

Photosynthetically available radiation (PAR or E, W m^{-2} for 400-700 nm) at a given depth is a function of light attenuation due to optical properties of seawater, self-shading by phytoplankton, and self-shading by macroalgae. For *Macrocystis pyrifera*, studies have found that light-attenuation within canopies is primarily due to self-shading resulting in depth-dependent photosynthetic activity (Gerard 1984; Edwards and Kim 2010).

Equation 22

$$E(z) = E_0 exp\left(k_w z + k_{chl-a}\int_z^{surface} chl - a(z')dz' + k_{N_f}\int_{z-1}^{surface} N_f(z-1')dz'\right)$$

E_0 is the PAR incident on the water surface and is provided as a boundary condition; k_w is the attenuation of light due to the optical properties of seawater (0.0384 m^{-1}; Lorenzen 1972); k_{chl-a} is shading specific to chl-a (0.0138 m^2 mg^{-1} chl-a; Lorenzen 1972); K_{Nf} is nitrogen-specific shading by the macroalgae (Table 6; m^2 mg^{-1} N; Hadley et al. 2015).

Farm Characteristics

Farm Dimensions

For longline-based designs of macroalgal farming we have defined six farm parameters that establish the size of the farm as well as the spatial distribution of macroalgae within the farm.

Table 5. Farm design parameters

Farm Variable	Description	"Base Case" Farm
Backbone Length	Length of the long line	400 m
Backbone Spacing	Distance between parallel long lines	26 m
No. of Backbones	Number of repeated long lines	15
Growth Line Length	Length of growth lines on the backbone	8 m
Growth Line Spacing	Spacing of growth lines on the backbone	2 m
Cultivation Depth	Depth below surface of backbone lines	20 m
Farm Orientation	Direction of farm relative to dominant flow direction	136°

The farm dimension in the x-direction is the total length of the backbone. The farm dimension in the y-direction is the total number of backbones times the spacing between the backbones. In the *MAG* model, there is an added buffer in the x- and y- dimension to allow for redistribution of the canopy at the surface that is beyond the extent of the edge of the backbones (e.g., 10 m). There is also an added buffer in the z-dimension to allow for the upwelling or downwelling of nutrients from below the cultivation depth (e.g., 10 m).

Farm orientation is a term that rotates incoming seawater velocities so that the dominant flow direction can either be, for example, parallel or perpendicular to backbones (Figure 5).

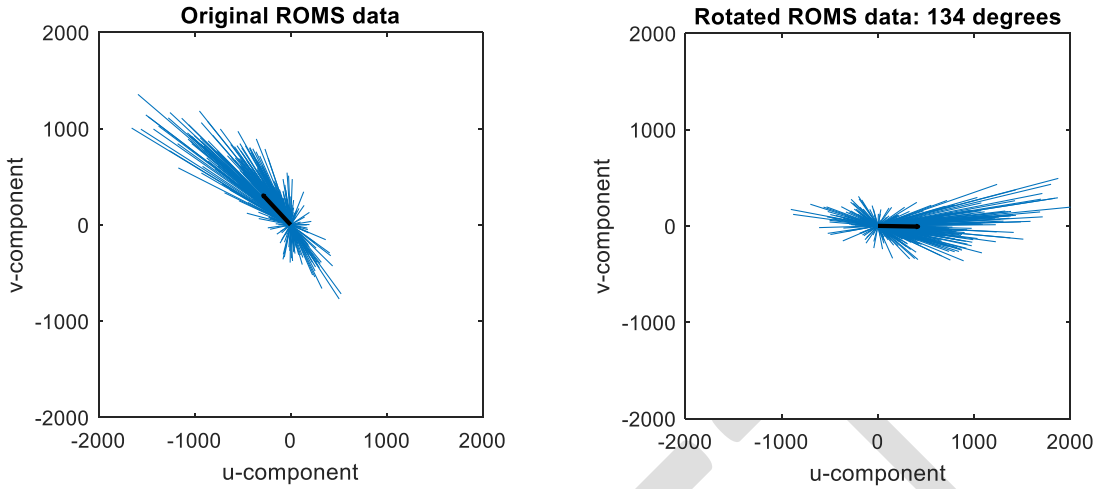

Figure 5. Orientation of farm relative to dominant flow

(Figure 5) Data from ROMS 1-km horizontal resolution simulation at the Santa Barbara farm location. (Left) Unrotated ROMS horizontal flow and (Right) rotated ROMS horizontal flow such that dominant flow is parallel to farm backbones.

Spatial and Temporal Resolution

The spatial resolution of the *MAG* model is 1 m^3 (dx = dy = dz) but see Appendix for notes on coarsening of the spatial resolution for the transport of nutrients through the farm.

There are three scales of temporal resolution in the *MAG* model (i.e., different processes are being resolved at different timescales). The time step for the transport function ($dt_{transport}$) is on the scale of seconds (see Appendix; $dt_{transport}$ adjusted based on spatial resolution to maintain stability). The time step for the uptake function (dt_{uptake}) is on the scale of hours. This allows for feedback between modified nutrient fields that occur on the scale of hours and kinetically limited uptake of nutrients by macroalgae (e.g., Michaelis-Menten uptake). The time step for the growth function (dt_{growth}; e.g., determination of ΔN_s and ΔN_f) is set to correspond with the temporal resolution of the ROMS boundary conditions (e.g., daily).

Farm Initiation

Farms are initiated by "seeding" an initial amount of biomass along the growth lines in the model. The initial amount of biomass is equivalent to a single meter-long frond per m^2. The date at which farms are initiated is an important parameter, typically optimal between November and February. This type of seeding assumes outplanting of sporophytes. The model could also be expanded to outplant gametophytes (i.e., with a "gameto-gun" as per pers. comm. J. Infante). This would require additional information regarding gametophyte-to-sporophyte transition rates and environmental cues.

Appendix

Numerical solution of nutrient transport

Diffusive and advective transport is a partial differential equation that describes the change in nutrient concentration in a given spatial domain over time. In three spatial dimensions, the nutrient transport equation can be written as:

Appendix Eq. 1

$$\frac{\partial C}{\partial t} = -\frac{\partial (uC)}{\partial x} - \frac{\partial (vC)}{\partial y} - \frac{\partial (wC)}{\partial z} + \frac{\partial}{\partial x}\left[\frac{\partial (D_h C)}{\partial x}\right] + \frac{\partial}{\partial y}\left[\frac{\partial (D_h C)}{\partial y}\right] + \frac{\partial}{\partial z}\left[\frac{\partial (D_v C)}{\partial z}\right]$$

where x, y and z (meters) are the spatial coordinates; u, v and w (m s^{-1}) are velocities in the x, y, and z direction; D_h and D_v are turbulent diffusion coefficients. Because of the parabolic nature of diffusion, the numerical solution applied is fully implicit for diffusion. The solution for advection is fully explicit due to its hyperbolic nature. An alternating direction implicit (ADI) method is implemented to solve for the 3-D nutrient transport. ADI in 3-D is a 3-step process. One dimension is solved at a time and each produce intermediate nutrient fields, C* and C** (in this case, x-direction, then y-direction, and then z-direction).

The discretization scheme applied to diffusion is first-order central differencing and to advection is upwind differencing after an evaluation of flow. The three discretized equations are:

*Appendix Eq. 2, x-implicit: Determine intermediate nutrient field C**

$$\begin{aligned}(-B_x)C^*_{-x} + (1+2B_x)C^* + (-B_x)C^*_{+x} \\ = \left(1 - A_x - A_y - A_z - 2B_y - 2B_z\right)\mathrm{C} + A_x C_{-x\ or\ +x} + A_y C_{-y\ or\ +y} + A_z C_{-z\ or\ +z} \\ + B_y C_{-y} + B_y C_{+y} + B_z C_{-z} + B_z C_{+z}\end{aligned}$$

*Appendix Eq. 3, y-implicit: Determine C***

$$\begin{aligned}\left(-B_y\right)C^{**}_{-y} + \left(1+2B_y\right)C^{**} + \left(-B_y\right)C^{**}_{+y} \\ = \left(1 - A_x - A_y - A_z - 2B_z\right)\mathrm{C} + A_x C_{-x\ or\ +x} + A_y C_{-y\ or\ +y} + A_z C_{-z\ or\ +z} + B_z C_{-z} \\ + B_z C_{+z} + B_x C^*_{-x} - 2B_x C^* + B_x C^*_{+x}\end{aligned}$$

Appendix Eq. 4, z-implicit: Determine C^{new}

$$\begin{aligned}(-B_z)C^{new}_{-z} + (1+2B_z)C^{new} + (-B_z)C^{new}_{+z} \\ = \left(1 - A_x - A_y - A_z\right)\mathrm{C} + A_x C_{-x\ or\ +x} + A_y C_{-y\ or\ +y} + A_z C_{-z\ or\ +z} + B_z C_{-z} + B_z C_{+z} \\ + B_x C^*_{-x} - 2B_x C^* + B_x C^*_{+x} + B_y C^{**}_{-y} - 2B_y C^{**} + B_y C^{**}_{+y}\end{aligned}$$

where the advection and diffusion terms are defined as:

Appendix Eq. 5

$$A_x = u_x \Delta t / 2\Delta x$$

$$A_y = u_y \Delta t / 2\Delta y$$

$$A_z = u_z \Delta t / 2\Delta z$$

$$B_x = D_h \Delta t / \Delta x^2$$

$$B_y = D_h \Delta t / \Delta y^2$$

$$B_z = D_v \Delta t / \Delta z^2$$

Δt is the temporal resolution (seconds); Δx, Δy and Δz (meters) are the spatial resolutions; and the subscripts $-x$, $-y$, $-z$, $+x$, $+y$, $+z$ refer to one positive or negative step in each spatial direction with respect to the location of C and C^{new}. D_h *and* D_v are horizontal and vertical diffusivity, respectively, and u is the advective velocity, both of which can be spatially heterogeneous.

Note that for Appendix Eq. 2, Appendix Eq. 3, and Appendix Eq. 4 the unknowns and knowns are written on the left and right-hand side of the equation respectively. The RHS is solved directly and the LHS is solved with a Thomas algorithm to obtain the unknown nutrient values.

Boundary Conditions: The above calculation can be made on all interior data points in the spatial domain. For boundaries at x = 1, end; y = 1, end; and z = end we apply a Dirichlet Boundary Condition where nutrient conditions are known (derived from ROMS simulation). At z = 1 (surface), a zero-gradient Neumann Boundary Conditions is applied (– x = + x).

Temporal and spatial resolution: The transport function in *MAG* has been evaluated to optimize spatial resolution yet minimize computational effort such that *MAG* simulations can be carried out for a year, plus. The spatial resolution of the macroalgal growth model is m^3, but the transport function can be coarsened up to a Δx and Δy of 10 m (Δz = 1m), and the temporal resolution, Δt, can then be relaxed up to 60 sec while maintaining stability in the transport function.

Table 6. Parameters for the macroalgal growth model

Variable	Description	Units	Value	Lower	Upper	Reference	Comment
$V_{max\ NO3}$	Maximum uptake rate of nitrate	µmol N m^{-2} h^{-1}	752	528	950	Gerard 1982	Based on combined results from Gerard 1982, Haines and Wheeler 1978
$V_{max\ NH4}$	Maximum uptake rate of ammonium	µmol N m^{-2} h^{-1}	739	665	813	Haines and Wheeler 1978	No data; 10% uncertainty applied
$V_{max\ Urea}$	Maximum uptake rate of urea	µmol N m^{-2} h^{-1}	12	n.d.	n.d.	Smith et al. 2018	Avg. based on max observed rate in Smith et al. 2018 converted to surface area
$K_{m\ NO3}$	Half saturation constant of nitrate	µmol N m^{-3}	10200	2000	14500	Brzezinski et al. 2013	Based on combined results from Gerard 1982, Haines and Wheeler 1978, Brzezinski et al. 2015
$K_{m\ NH4}$	Half saturation constant of ammonium	µmol N m^{-3}	5310	4310	6310	Haines and Wheeler 1978	1 S.E.; Haines and Wheeler 1978
$K_{m\ Urea}$	Half saturation constant of urea	µmol N m^{-3}	7755	n.d.	n.d.	n.d.	no data; value based on combined results of Nitrate and Ammonium
Q_{max}	Maximum internal nitrogen	mg N $g(dw)^{-1}$	40	36	44	Brzezinski et al. 2013	Max value observed at SBC LTER, Brzezinski et al. 2013
Q_{min}	Minimum internal nitrogen	mg N $g(dw)^{-1}$	10	7	11	Brzezinski et al. 2013	Bounds based on Hadley et al. 2015 (cites Lobban and Harrison 1994) and Gerard 1982 Marine Biology
μ_{max}	Maximum growth rate	d^{-1}	0.2	0.1	0.2	Rassweiler et al. 2018; Wheeler and North 1980	Max. value observed at SBC LTER; Max. value observed in Wheeler and North
T_{min}	Temperature-limited constant	°C	14	8	14	Zimmerman and Kremer 1986	Lower based on Buschmann et al. 2004; range of temperatures in Chile
T_{max}	Temperature-limited constant	°C	20	19	23	Zimmerman and Kremer 1986	Upper based on Buschmann et al. 2004; range of temperatures in Chile
T_{lim}	Temperature-limited constant	°C	23	20	25	Schiel and Foster 2015	Lower based on juvenile performance, Setchell 1932
k_{PAR}	Light-limited growth constant		-0.333	-0.3000	-0.3667	Dean and Jacobsen 1985	No data; 10% uncertainty applied
PAR_c	Light-limited compensating irradiance	W m^{-2}	1.7864	1.6078	1.9650	Dean and Jacobsen 1985	No data; 10% uncertainty applied

k_{Nf}	Light attenuation due to macroalgae	$m^2\ mg^{-1}\ N_f$	0.0001	0.00009	0.00011	Hadley et al. 2015	No data; 10% uncertainty applied
h_{max}	Maximum attainable frond height	m	30	25	30	D. Seigel pers. comm.	No data; 10% uncertainty applied
S_i	Frond initiation rate	d^{-1}	0.0106 * Q + 0.018	0.005	0.40	Rodriguez et al. 2013; Bell et al. 2018	Relationship based on Bell et al. 2018, Fig. S2 and Chl:C vs %N relationship (T. Bell, pers. comm.)
Age_{max}	Maximum frond age	d	150	75	150	Rodriguez et al. 2013	Data bounds based on Rodriguez et al. 2013
E	Exudation rate	d^{-1}	0.002	0.001	0.003	Rassweiler et al. 2018	Avg based on all data from Rassweiler et al. 2018 ± 1 S.D.
d_{wave}	Wave-dependent mortality	d^{-1}	0.010915 × H_S	0.00970	0.0121	Rodriguez et al. 2013	[h-1] 0.000455 * Hs; set the intercept to zero; [0.000404, 0.000506]
d_{blade}	Blade loss rate	d^{-1}	0.009	0.007	0.011	Rassweiler et al. 2018	Avg based on all data from Rassweiler et al. 2018 ± 1 S.D.
d_{frond}	Frond loss rate, post-mortality	d^{-1}	0.1	0.09	0.11	n.d.	No data; 10% uncertainty applied